AJNR

This information is current as of February 26, 2026.

Prevalence of Rathke Cleft and Other Incidental Pituitary Gland Findings on Contrast-Enhanced 3D Fat-Saturated T1 MPRAGE at 7T MRI

Mikael Mir, Nathaniel P. Miller, Matthew White, Wendy Elvandahl, Ayca Ersen Danyeli and Can Özütemiz

AJNR Am J Neuroradiol 2024, 45 (11) 1811-1818
doi: https://doi.org/10.3174/ajnr.A8393
http://www.ajnr.org/content/45/11/1811

Prevalence of Rathke Cleft and Other Incidental Pituitary Gland Findings on Contrast-Enhanced 3D Fat-Saturated T1 MPRAGE at 7T MRI

Mikael Mir, Nathaniel P. Miller, Matthew White, Wendy Elvandahl, Ayca Ersen Danyeli, and Can Özütemiz

ABSTRACT

BACKGROUND AND PURPOSE: A cleftlike nonenhancing hypointensity was observed repeatedly in the pituitary gland at the adenohypophysis/neurohypophysis border on contrast-enhanced 3D fat-saturated T1-MPRAGE using clinical 7T MRI. Our primary goal was to assess the prevalence of this finding. The secondary goals were to evaluate the frequency of other incidental pituitary lesions, MRI artifacts, and their effect on pituitary imaging on the contrast-enhanced 3D fat-saturated T1 MPRAGE at 7T.

MATERIALS AND METHODS: One hundred patients who underwent 7T neuroimaging between October 27, 2021, and August 10, 2023, were included. Each case was evaluated for cleftlike pituitary hypointensity, pituitary masses, and artifacts on contrast-enhanced 3D fat-saturated T1 MPRAGE. Follow-up examinations were evaluated if present. The average prevalence for each finding was calculated, as were descriptive statistics for age and sex.

RESULTS: A cleftlike hypointensity was present in 66% of 7T MRIs. There were no significant differences between the "cleftlike present" and "cleftlike absent" groups regarding sex ($P = .39$) and age ($P = .32$). The cleftlike hypointensity was demonstrated on follow-up MRIs in 3/3 patients with 7T, 1/12 with 3T, and 1/5 with 1.5T. A mass was found in 22%, while 75% had no mass and 3% were indeterminate. A mass was found in 18 (27%) of the cleftlike present and 4 (13%) of the cleftlike absent groups. The most common mass types were Rathke cleft cyst in 7 (31.8%) patients, "Rathke cleft cyst versus entrapped CSF" in 6 (27.3%), and microadenoma in 6 (22.2%) in the cleftlike present group. There were no significant differences in the mass types between the cleftlike present and cleftlike absent groups ($P = .23$). Susceptibility and/or motion artifacts were frequent using contrast-enhanced 3D fat-saturated T1 MPRAGE (54%). Artifact-free scans were significantly more frequent in the cleftlike present group ($P = .03$).

CONCLUSIONS: A cleftlike nonenhancing hypointensity was frequently seen on the contrast-enhanced 3D fat-saturated T1 MPRAGE images at 7T MRI, which most likely represents a normal embryologic Rathke cleft remnant and cannot be seen in lower-field-strength MRIs. Susceptibility and motion artifacts are common in the sella. They may affect image quality, and the artifacts at 7T may lead to an underestimation of the prevalence of the Rathke cleft and other incidental findings.

ABBREVIATIONS: C+3D FS T1 MPRAGE = contrast-enhanced 3D fat-saturated T1 MPRAGE; FS = fat-saturated; RCC = Rathke cleft cyst

The FDA has approved 7T MRI machines for clinical knee and brain imaging using dedicated coils.[1-3] 7T MRI technology offers several advantages over conventional 1.5 and 3T MRI systems, including a higher SNR and contrast-to-noise ratio, which provide MR images with better spatial resolution, improving discrimination of smaller lesions and anatomy.[3-6] Conversely, 7T MRI technology brings new challenges. The primary limitations in clinical 7T neuroimaging are transit B_1 field inhomogeneities and increased susceptibility effects, which limit imaging of the skull base.[3-5,7-13] Another limitation is increased sensitivity to motion and pulsation artifacts.[3,9,10] Despite these limitations, 7T MRI has been shown to detect small pituitary microadenomas, occult on conventional pituitary MRI at lower field strengths.[3,14-18]

7T MRI has been used at our center since 2020 for various indications, including pituitary imaging. We routinely obtain a sagittally acquired contrast-enhanced 3D fat-saturated T1 MPRAGE (C + 3D FS T1 MPRAGE) with axial and coronal reformats for postcontrast brain imaging at 7T, which is the main contrast-enhanced sequence we use to evaluate contrast-enhancing intracranial pathologies. In our daily practice, we have repeatedly observed a cleftlike J-shaped or C-shaped nonenhancing hypointensity in

Received April 11, 2024; accepted after revision June 15.

From the University of Minnesota Medical School (M.M., N.P.M.), Minneapolis, Minnesota; Center for Magnetic Resonance Research (M.W., W.E.), University of Minnesota, Minneapolis, Minnesota; Department of Pathology (A.E.D.), School of Medicine, Acıbadem University, Istanbul, Turkey; and Department of Radiology (C.Ö.), University of Minnesota Medical School, Minneapolis, Minnesota.

Please address correspondence to Can Özütemiz, MD, Department of Radiology, University of Minnesota MMC 292, 420 Delaware St. SE Minneapolis, MN 55455; e-mail: ozutemiz@umn.edu; @CanOzutemiz; @UMNRadiology

http://dx.doi.org/10.3174/ajnr.A8393

SUMMARY

PREVIOUS LITERATURE: 7T MRI offers better spatial resolution, which has improved discrimination of small lesions and anatomy. In our daily practice, we have repeatedly observed a cleftlike J-shaped or C-shaped nonenhancing hypointensity in the pituitary gland at the adenohypophysis/neurohypophysis border on sagittal C + 3D FS T1 MPRAGE at 7T. Gobara et al[26] observed a beltlike T2 hypointensity in the posterior margin of the adenohypophysis in 37.7% of 212 cases on T2-weighted images at 3T MRI, and the investigators postulated that this represented "pars intermedia" or Rathke cleft remnant. This benign embryologic remnant can further develop into a large Rathke cleft cyst.

KEY FINDINGS: A cleftlike pituitary hypointensity was present in 66/100 (66%) patients. This incidental finding was demonstrated in 3/3 patients with 7T, 1/12 with 3T, and 1/5 with 1.5T follow-up. A pituitary mass was found in 22%, and susceptibility and/or motion artifacts were generally frequent (54%) when using C + 3D FS T1 MPRAGE at 7T.

KNOWLEDGE ADVANCEMENT: A cleftlike nonenhancing hypointensity is frequently present on C + 3D FS T1 MPRAGE at 7T MRI. This is likely benign Rathke cleft remnant and cannot be seen in lower-field-strength MRIs. Susceptibility and motion artifacts are common in the sella, which may affect image quality at 7T.

the pituitary gland at the border of the adenohypophysis and neurohypophysis on the C + 3D FS T1 MPRAGE sequence, best appreciated in the sagittal plane. In this study, our primary goal was to determine the prevalence of this finding and assess whether it is visualized on follow-up MRIs with either 7T or lower field strengths. Our second goal was to evaluate the frequency of other incidental pituitary gland lesions, MRI artifacts, and their effect on pituitary imaging on the C + 3D FS T1 MPRAGE sequence at 7T.

MATERIALS AND METHODS

This study protocol was approved by the institutional review board at the University of Minnesota. Given the retrospective nature of the study, the institutional review board granted a waiver for informed consent.

Image Acquisition and Interpretation

Images and demographic data from 175 patients who underwent neuroimaging with an FDA-approved clinical 7T MRI scanner (Magnetom Terra; Siemens) equipped with a 1-channel transmit/32-channel receive head coil (Nova Medical) at the Center for Magnetic Resonance Research in Minneapolis, Minnesota, between October 27, 2021, and August 10, 2023, were collected for this study. Our C + 3D FS T1 MPRAGE sequence parameters are shown in Table 1. A half-dose (0.05 mL/kg) of standard gadolinium-based contrast agent (Gadavist; Bayer) is used routinely for each 7T MRI examination at our center. Commercially available (Multiwave Imaging, Marseille, France) and in-house-made calcium titanate dielectric pads were placed in the suboccipital and pre-auricular regions, depending on the patient's head size. We specifically apply these pads because transmit B_1 inhomogeneities may limit the visibility of nearby structures at the cranium base with 7T, and dielectric pads were proved to decrease these effects.[3,11,19,20] We collected the following clinical data: age, sex, and examination indication.

Table 1: C + 3D FS T1 MPRAGE sequence parameters

Parameter	Value
Plane	Sagittal
Slice thickness (mm)	0.6
Matrix	224 × 224
FOV (mm)	150
Interslice distance (%)	50
Voxel size (mm^3)	0.3 × 0.3 × 0.3[a]
Acquisition time (min)	6:32
TR/TE (ms)	3000/2.49

[a] In our contrast-enhanced radiation therapy protocol, the interpolation is off to decrease geometric distortion, and therefore the voxel size is 0.6 × 0.6 × 0.6 mm^3.

Each case was evaluated for 2 findings on C + 3D FS T1 MPRAGE: a cleftlike J-shaped or C-shaped nonenhancing pituitary hypointensity at the border of the adenohypophysis and neurohypophysis ("cleftlike present") and a pituitary gland mass, scored as absent, present, or indeterminate. The presence of a posterior pituitary T1 bright spot, consistent with neurohypophysis, was assessed in the precontrast and postcontrast MPRAGE series, and it was scored as absent, present, indeterminate, or ectopic. The presence and type of artifacts seen on C + 3D FS T1 MPRAGE were also recorded. Data from those with prior or follow-up scans were collected as well. The voxel size of our institutional C + 3D FS T1 MPRAGE at 1.5T and 3T MRI is 1 × 1× 1 mm.

Data Analysis and Statistics

After an initial training session, which included 20 cases provided by a board-certified neuroradiologist (6 years of experience and >2 years of experience reading a high volume of clinical 7T MRI cases), 2 medical students evaluated and assessed all 175 7T MRI examinations. Seventy-three cases were excluded due to a lack of C + 3D FS T1 MPRAGE sequence, and two cases were excluded due to motion artifacts that limited interpretation from the final analysis. In the end, a total of 100 MRIs were included. Then, the attending neuroradiologist separately reviewed and controlled all included cases in a separate session, either agreeing or disagreeing with the medical students to reach a final consensus agreement.

The average and SD for each of the 3 findings were calculated from the remaining cases and descriptive statistics for age, sex, protocol, and indication. To assess differences in baseline demographic characteristics between the cleftlike present and cleftlike absent groups, we performed a χ^2 test to evaluate differences in sex and an unpaired, 2-tailed t test to evaluate differences in

Table 2: 7T MRI indications

Indication	(No.) (%)
Epilepsy	10 (10%)
Headache	10 (10%)
Multiple Sclerosis	8 (8%)
Pituitary adenoma	8 (8%)
Seizure	6 (6%)
Pituitary lesion	5 (5%)
Assess for CAA	4 (4%)
Brain lesion	4 (4%)
Radiation therapy planning	4 (4%)
Cushing disease	3 (3%)
Gait disorder	3 (3%)
Radiation therapy planning for glioblastoma	3 (3%)
Glioblastoma	3 (3%)
Memory changes	3 (3%)
Stroke/TIA	3 (3%)
Vision changes	3 (3%)
Dizziness	2 (2%)

Note:—CAA indicates Cerebral Amyloid Angiopathy.

patient age. Additional χ^2 testing was conducted to assess differences in the type of masses and the presence and type of artifacts in the 2 groups. A subgroup analysis was performed for patients with follow-up C + 3D FS T1 MPRAGE at any field strength.

RESULTS

Among the 100 patients included, 64 were women and 36 were men, with an average age of 47.3 (SD, 18.9) years. The indications for each study used in the cohort are shown in Table 2.

A cleftlike pituitary hypointensity was present in 66 (66%) patients, absent in 31 (31%), and indeterminate in 3 (3%) (Figs 1–3). Indeterminate cases were excluded from subsequent analyses. For the cleftlike present group, 41 (62%) were women, and 25 (38%) were men, with an average age of 46.1 (SD, 19.9) years. For the cleftlike absent group, 22 (71%) were women and 9 (29%) were men, with an average age of 50.3 (SD, 17.1) years. There were no significant differences in the baseline characteristics of the cleftlike present and cleftlike absent groups regarding sex [$\chi^2(1, n = 97) = 0.73$, $P = .39$] or age (2-tailed t test, $P = .32$). In the cleftlike present group, 20 patients underwent follow-up imaging. A cleftlike hypointensity in the pituitary gland was demonstrated in 3/3 patients with 7T, 1/12 with 3T, and 1/5 with 1.5T follow-up (Figs 2 and 3).

A masslike appearance in the pituitary gland was found in 22 (22%) patients, while 75 (75%) had no mass and 3 (3%) were indeterminate. The most common types of masses in the cleftlike present group were Rathke cleft cyst (RCC) in 7 (31.8%) patients, "RCC-versus-entrapped CSF" in 6 (27.3%), and pituitary adenoma in 4 (18.2%). In the cleftlike absent group, only 20% of patients had an RCC-versus-entrapped CSF-like appearance, and no RCC was identified radiologically. Some patients had 2 masses noted on their interpretation, and the prevalence of all masses noted is shown in Table 3. There was no significant difference in the types of mass present in the cleftlike present and cleftlike absent groups [$\chi^2(6, n = 27) = 8.06$, $P = .23$]. A posterior T1 bright spot was present in 93 (93%) patients, absent in 3 (3%), indeterminate in 3 (3%), and ectopic in 1 (1%) at the stalk. A posterior T1 bright spot was present in the expected area in 94% of patients in the cleftlike present group (62/66) and 94% in the cleftlike absent (29/31).

Regarding artifacts, 54 (54%) patients had some type of artifact noted in the

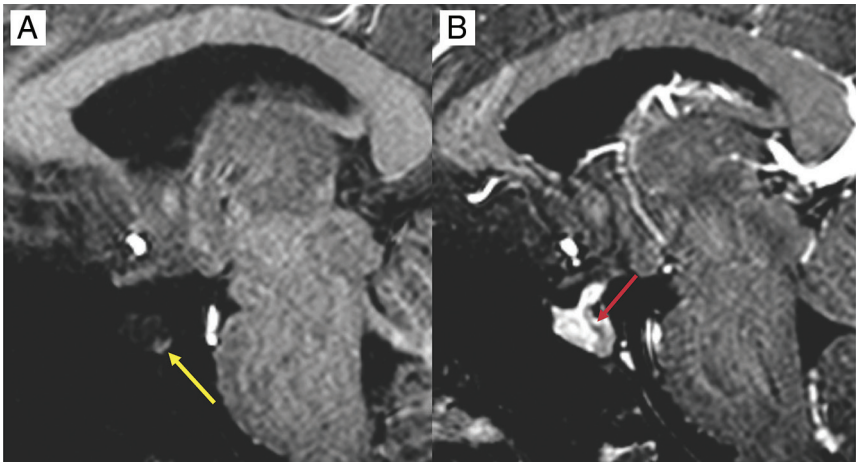

FIG 1. A 32-year-old woman who was scanned for multiple sclerosis follow-up. *A*, Precontrast 3D FS T1 MPRAGE shows a very dark adenohypophysis and stalk. A posterior T1 bright spot is present (*yellow arrow*). *B*, Postcontrast image shows diffuse homogeneous enhancement of the stalk, adenohypophysis, and an incidental curved nonenhancing hypointensity (*red arrow*), extending from the stalk between the vicinity of adenohypophysis and neurohypophysis, presumably representing the Rathke cleft.

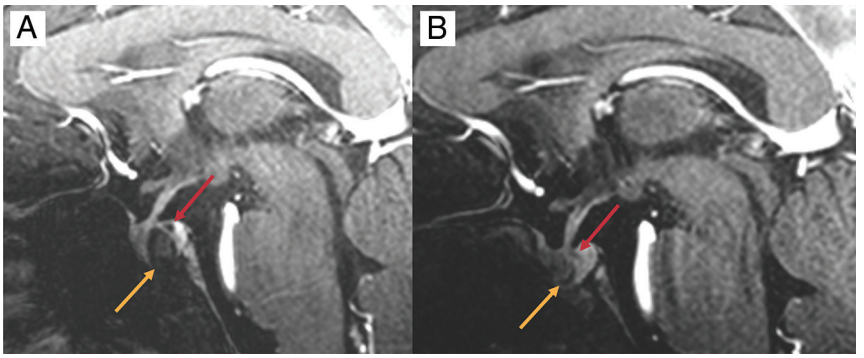

FIG 2. *A*, A 30-year-old man with pituitary hypofunction. On a sagittal postcontrast 3D FS T1 MPRAGE at 7T, the *orange arrow* shows a biopsy-proved large RCC, and the *red arrow* shows a separate triangular hypointensity more posterior and superior to the cyst. *B*, A 3-month follow-up with 7T MRI after endoscopic transsphenoidal drainage of the cyst shows a decompressed RCC (*orange arrow*) and a more dilated and prominent appearance of the J-shaped cleftlike presumed Rathke cleft (*red arrow*), likely due to resolution of the mass effect. The pituitary hypofunction resolved after the surgery.

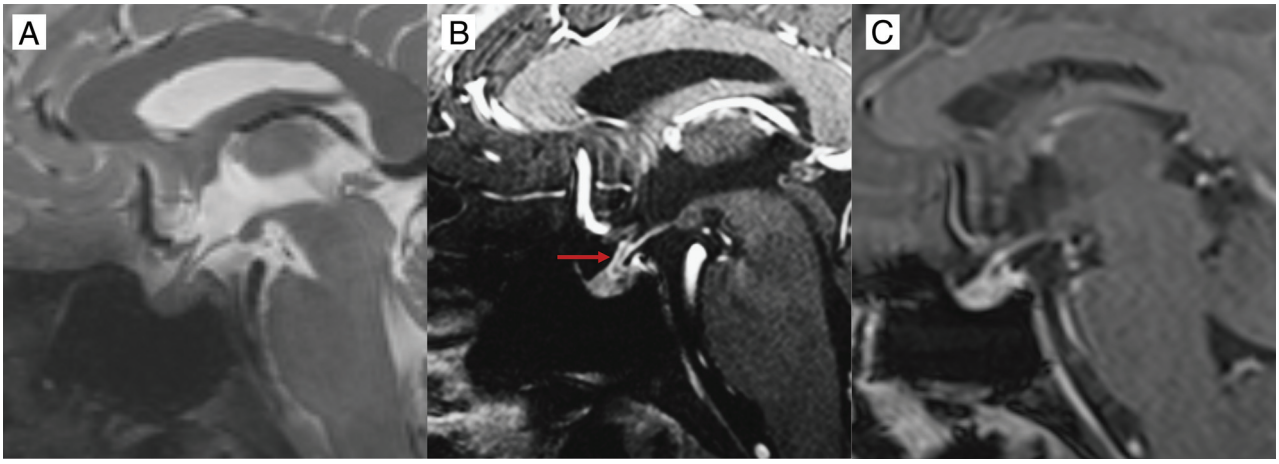

FIG 3. A 37-year-old man with medically refractory epilepsy and prior temporal lobectomy was referred to 7T MRI for follow-up. *A*, Sagittal precontrast 3D-T2-SPACE image does not show any abnormality in the pituitary gland, and the lesion indicated by the *red arrow* in *B* is not visible. *B*, Sagittal postcontrast 3D FS T1 MPRAGE at 7T shows a string-like C-shaped hypointensity extending from the stalk all the way through the adenohypophysis (*red arrow*), favored as a Rathke cleft. *C*, Sagittal contrast-enhanced 3D T1 MPRAGE image obtained 5 months later at 3T MRI are unable to demonstrate the presumed Rathke cleft.

Table 3: Frequency of pituitary masses

Mass Type	Total (No.) (%)	Cleftlike Present (No.) (%)	Cleftlike Absent (No.) (%)
RCC	7 (25.9%)	7 (31.8%)	0
RCC vs entrapped CSF	7 (25.9%)	6 (27.3%)	1 (20%)
RCC vs entrapped CSF vs adenoma	2 (7.4%)	2 (9.1%)	0
Entrapped CSF	3 (11.1%)	1 (4.5%)	2 (40%)
Adenoma	6 (22.2%)	4 (18.2%)	2 (40%)
Drained RCC without mass effect	1 (3.7%)	1 (4.5%)	0
Adenoma vs artifacts	1 (3.7%)	1 (4.5%)	0
Total (frequency)	27	22	5

Table 4: Prevalence of artifacts[a]

Artifact	Total (No.) (%)	Cleftlike Present (No.) (%)	Cleftlike Absent (No.) (%)
Present	57 (58.8%)	34 (51.5%)	23 (74.2%)
Absent	40 (41.2%)	32 (48.5%)	8 (25.8%)
Total (patients)	97	66	31
Artifact type			
Motion	30 (41.1%)	19 (44.2%)	11 (36.7%)
Susceptibility	43 (58.9%)	24 (55.8%)	19 (63.3%)
Total	73	43	30

[a] Overall presence of artifacts across patients ($n = 97$, three omitted), reported in total and for Cleftlike Present and Cleftlike Absent groups. A statistically significant difference between Cleftlike Present and Cleftlike Absent groups, with a proportionately higher rate of scan artifacts in the Cleftlike Absent group [$\chi^2(1, n = 97) = 4.48$, $P = .03$]. Below are subgroup frequencies of artifact types. Note that the lower rows report artifact frequencies across studies, not by the patient (some scans include both susceptibility and motion artifacts). No statistically significant difference was found in types of artifacts between Cleftlike Present and Cleftlike Absent groups [$\chi^2(1, n = 73) = 0.41$, $P = .52$].

C + 3D FS T1 MPRAGE scan, and the prevalence of artifacts within the cohort is outlined in Table 4.

DISCUSSION

Our results characterize a previously unreported cleftlike J-shaped or C-shaped nonenhancing pituitary hypointensity found on C + 3D FS T1 MPRAGE in most patients scanned at 7T. This finding was specifically localized between the T1 hyperintense neurohypophysis and the adenohypophysis, which appears T1 hypointense on the precontrast series and homogeneously enhancing on the postcontrast series (Fig 1). While this incidental observation was repeatedly noted in a small group of patients with available follow-up at 7T, it was not appreciated in most cases with lower-field-strength follow-ups or could be identified in the lower field strengths only after initially seeing the lesion at 7T. This incidental imaging finding presumably represents a tiny true anatomic structure that is only visible with 7T and obscured in lower field strengths due to relatively lower spatial and contrast resolution. The frequency of this J-shaped cleftlike hypointensity may also be underestimated in our series, because a significantly greater proportion of patients in the cleftlike absent group had artifact-degraded studies, which may have limited visualization.

After correlation with histopathologic examinations from cadavers and pituitary tumor resections, we concluded that this cleftlike hypointensity presumably represents a Rathke cleft, an embryologic remnant of the Rathke pouch (Fig 4), seen as a normal anatomic structure between the pars intermedia and pars distalis, which is not typically observed in lower-strength studies.[21-24] Embryologically, the Rathke pouch is derived from the ectodermal buccopharyngeal membrane and grows dorsally at around 3 weeks of gestation. At approximately 32 days, this structure is disconnected from the oral cavity and communicates with the diencephalon. At the same time, the infundibular process grows from the diencephalon

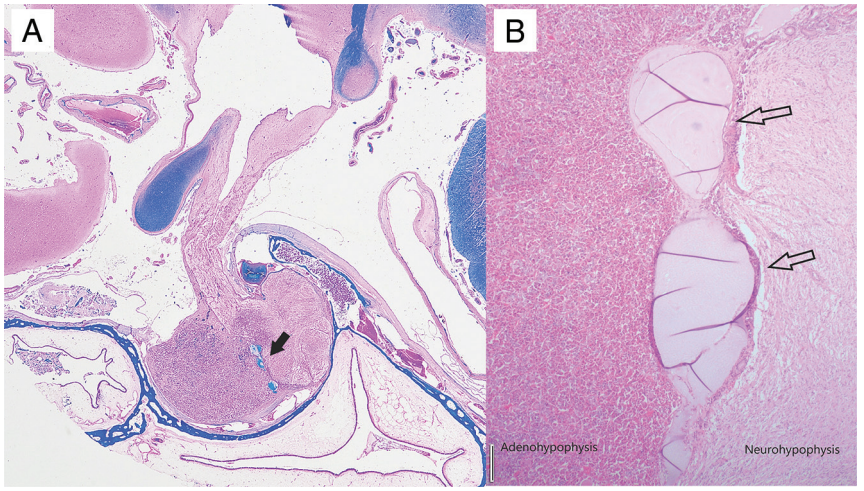

FIG 4. *A*, The whole-slide image from a postmortem case shows the pituitary gland along with anatomically adjacent tissues. The *arrow* indicates a Rathke cleft remnant (stained with Luxol fast blue combined with periodic acid-Schiff, ×0.5 magnification). *B*, The closer view depicts a Rathke cleft remnant (*arrows*) (stained with H&E, ×20 magnification).

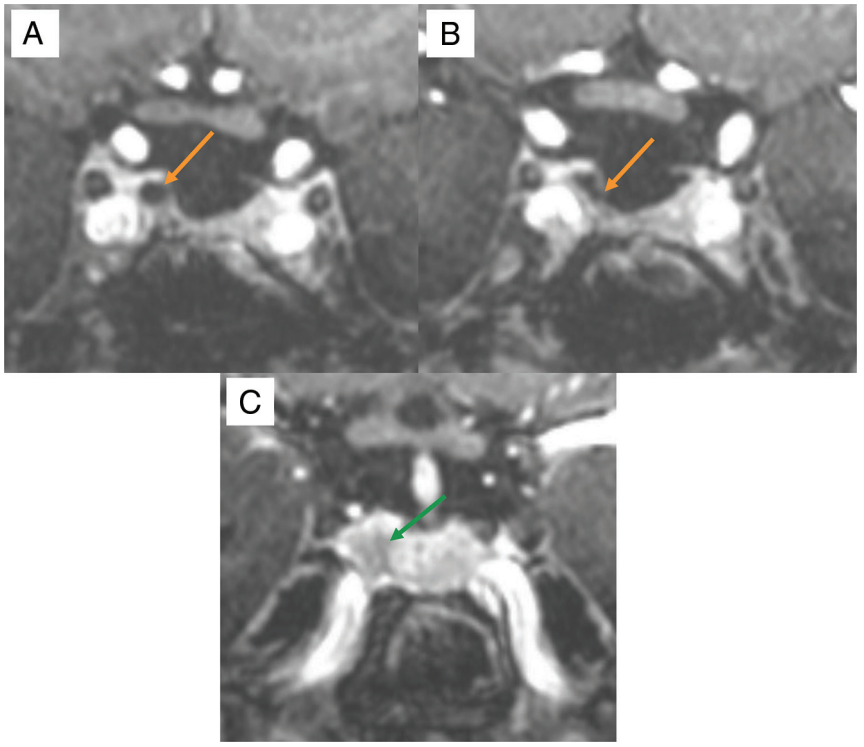

FIG 5. A 45-year-old woman with increased prolactin levels who had a transnasal endoscopic pituitary adenoma resection and underwent a follow-up with a 7T MRI due to increased prolactin levels 2 months after the operation. *A*, Coronal postcontrast 3D FS T1 MPRAGE shows a hypointense cystic structure mimicking a cystic adenoma located at the right ventral aspect of the adenohypophysis (*orange arrows*) with indistinct margins. *B*, When one scrolls posteriorly, the cystic mass connects with the CSF. Thus, this mass likely represents an entrapped CSF in the operation field. *C*, When scrolled even further in the posterior direction, there is a more hypointense focus with indistinct margins in the right aspect of the adenohypophysis, considered as a residual adenoma (*green arrow*).

inferiorly toward the buccal cavity to form the neurohypophysis and the stalk. The anterior wall of the Rathke pouch forms the adenohypophysis, and the posterior wall forms the pars intermedia.[21,22] Sometimes, the Rathke pouch leaves a remnant between the pars distalis and pars intermedia, known as the Rathke cleft, which can further develop into a large RCC.[21,22] Note that RCC and cyst of the pars intermedia are 2 terms used interchangeably in the literature, and a true differentiation of those two is unclear.

To our knowledge, the study of Gobara et al[26] is the only one with a similar and interesting observation. In this study, the investigators obtained high-resolution 2D T2 TSE images of the pituitary gland at 3T. They observed a T2 hypointensity in the posterior margin of the adenohypophysis in 37.7% of 212 cases, of which 37 (17.5%) showed a belt-like hypointensity on T2-weighted images, and the investigators postulated that this belt-like T2 hypointense radiologic observation represented the pars intermedia or a Rathke cleft remnant, similar to ours.[26] In our routine 7T MRI protocols, we do not acquire a high-resolution 2D TSE sequence focused on the pituitary gland. Thus, we did not analyze how the here-described cleftlike J-shaped/C-shaped nonenhancing hypointensity appeared on T2-weighted images. However, in our 7T study, the prevalence of this incidental finding is even higher compared with the findings of Gobara et al (66% versus 17.5%).

The prevalence of an RCC in our cohort was 7%. The true prevalence of RCCs in the general population is variable in the literature. Because symptomatic cases are rare, many RCCs are found postmortem. Postmortem studies suggest that the prevalence is between 13% and 23%, with some studies finding incidental lesions in 11% of postmortem cases.[27,28] Regarding the radiologic prevalence, the prevalence of RCC on MRI was found at 3% in the pediatric population, and 1 study performed in a tertiary pituitary center including all age groups found a prevalence of 3.4% in 2598 pituitary MRI cases using conventional 1.5 and 3T MRI machines.[29,30] The prevalence in our small cohort is greater than that in the latter radiology report, probably due to improved spatial and contrast resolution at 7T, but it is still less than the prevalence reported by the postmortem studies. Nevertheless, RCCs are benign incidental cysts that are often asymptomatic and only rarely cause endocrinologic dysfunction when they are sufficiently

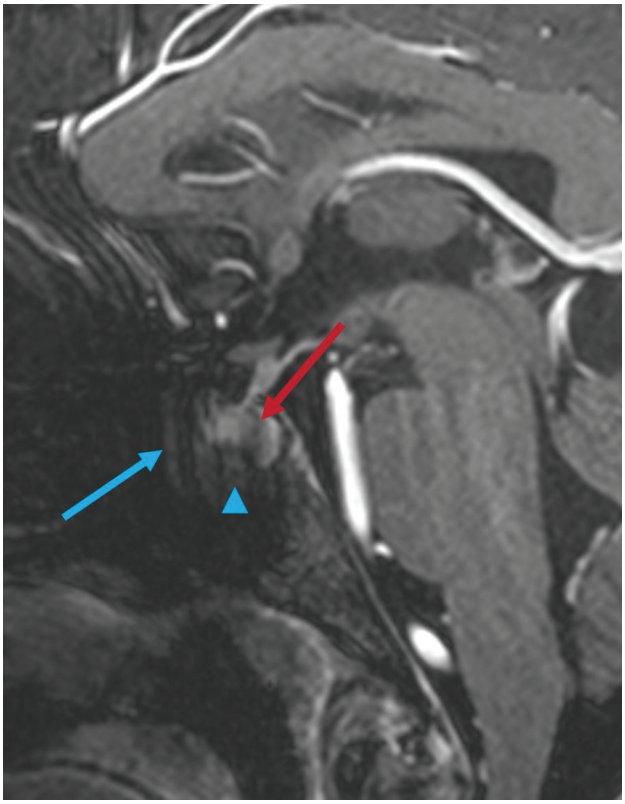

FIG 6. A 19-year-old woman was imaged for a low-grade brain tumor at 7T. While the cleftlike presumed Rathke cleft remnant can be depicted (*red arrow*), pulsation artifacts from the adjacent basilar artery (*blue arrow*) and susceptibility artifacts associated with sphenoid sinus (*blue arrowhead*) limit the assessment of the ventral and inferior portions of the pituitary gland.

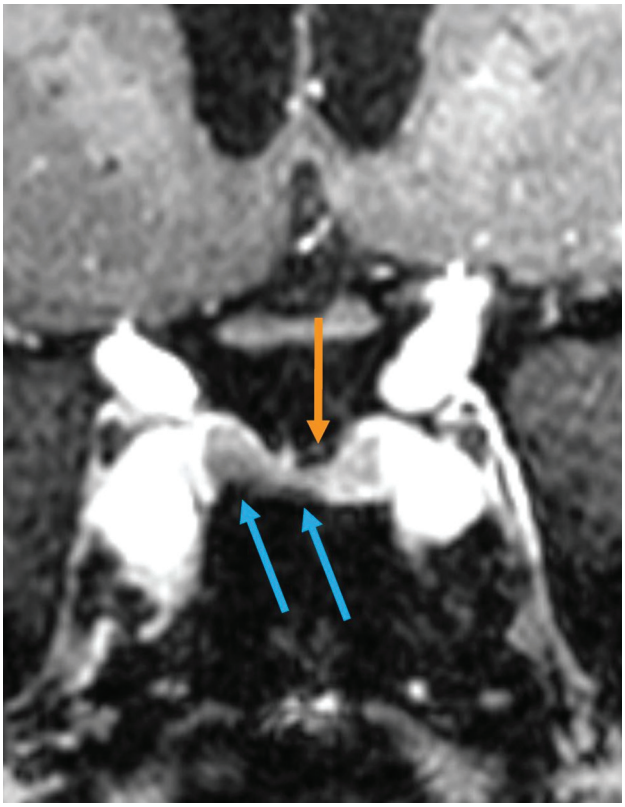

FIG 7. An 83-year-old woman who was referred for a brain MRI for a posterior communicating artery aneurysm follow-up. Coronal C + 3D FS T1 MPRAGE shows rounded susceptibility artifacts in the base of the adenohypophysis (*blue arrows*), which may mimic a hypointense adenoma and limit the assessment of the base. A cystic-appearing T1 hypointense area immediately lateral to the stalk and superior to the gland (*Orange arrow*) is separated by a thin membrane and is continuous with adjacent CSF in other slices (not shown). This is favored to represent entrapped CSF between the gland and the diaphragm, mimicking a cystic mass.

large to have a mass effect on adjacent structures.[25,31] Despite the lack of statistical difference, in almost one-quarter of the patients with cleftlike present, an RCC was present, while none in the cleftlike absent group had an RCC. This relationship increases the potential association between the visible Rathke cleft remnant and the RCC (Table 3).

It is known that an RCC may appear similar to a nonenhancing cystic pituitary adenoma, and radiologic differentiation is sometimes impossible.[22,24] With the improved resolution gained with 7T imaging, we could identify additional masslike structures in these C + 3D FS T1 MPRAGE sequences. One example is that we observed cystic masslike lesions which were presumed to represent either entrapped CSF underneath the diaphragma sellae or CSF-filled arachnoid indentations into the adenohypophysis. Unlike an RCC, these nonenhancing cystlike structures were almost always off the midline in unexpected locations for RCCs, either lateral or superolateral to the adenohypophysis, demonstrating a similar signal to CSF and usually contiguous with the CSF, as seen in Fig 5. As shown in Table 3, in a few cases, we were unable to differentiate the nature of the cyst. Therefore, we debated whether these were incidental nonenhancing adenomas, RCCs, or entrapped CSF. Because we are in the early stages of clinical use of 7T MRI, neuroradiologists are not used to the depiction of subtle pituitary pathologies at 7T, even in the most experienced institutions with high volumes of 7T MRI. Thus, it is important for those interpreting these studies to understand the appearance of Rathke cleft remnant, RCC, and other incidental benign cystic lesions, such as entrapped CSF underneath the diaphragma sellae or CSF-filled arachnoid indentations and to differentiate these from other pituitary lesions such as microadenomas, to avoid unnecessary follow-up laboratory testing and imaging for the patient.[31]

High-resolution postcontrast 3D T1 MPRAGE at 7T was recently found to be more successful in identifying pituitary microadenomas in a small cohort of patients with Cushing disease compared with other 3D, 2D, and dynamic sequences.[18] Sphenoid sinus pneumatization is also reported as a limiting factor because of increased susceptibility artifacts in the air-bone interphase.[18] Our institutional experience aligns with the report from this group. In most of the scans in our sample, some degree of artifact was noted, either motion-related or susceptibility artifacts, mainly occurring in the sella floor from the air-bone interphase or B_1 field inhomogeneities (Figs 6 and 7). Motion artifacts are a known problem with scans requiring a longer acquisition time, and it is known that artifacts are exaggerated at 7T compared with conventional MRIs at 1.5T and 3T.[3] There were significantly more artifact-free scans in the cleftlike

present group than in the cleftlike absent group, implying that the higher degree of artifacts in the cleftlike absent group could have limited our ability to identify the J-shaped or C-shaped cleftlike hypointensity. Thus, it is possible that the overall prevalence of the cleftlike hypointensity is relatively underestimated in our cohort (Table 4).

One of the limitations of this study is the lack of pathologic confirmation in our cohort. While this is potentially a limitation, within the limits of a retrospective study with incidental benign findings seen on 7T MRI, it is inhumane and impractical to perform pathologic confirmation. To decrease this limitation, we correlated our imaging with prior postmortem cases. A postmortem case in the future with available prior contrast-enhanced 7T MRI may confirm our findings. Another minor limitation is that all images were first assessed by medical students and their observations were corrected by a single experienced neuroradiologist; therefore, interobserver variability analysis was not performed.

CONCLUSIONS

A nonenhancing, J-shaped or C-shaped cleftlike hypointensity in the pituitary gland between the adenohypophysis and neurohypophysis is seen in most of the sagittal contrast-enhanced 3D fat-saturated T1 MPRAGE sequences at 7T MRI. We suggest that this radiologic observation represents a Rathke cleft, an embryologic Rathke pouch remnant, seen as a normal anatomic structure between the pars intermedia and pars distalis on histopathology but cannot be seen clearly on lower-field-strength MRIs. The artifacts at 7T are a limiting factor, and perhaps the overall prevalence of this cleftlike hypointensity is underrepresented due to the artifacts limiting interpretation. Additionally, 7T MRI may further capture incidental benign cystic pituitary lesions, such as presumed entrapped CSF under the diaphragma sellae or arachnoid indentations into the adenohypophysis, in unexpected locations for RCC.

Disclosure forms provided by the authors are available with the full text and PDF of this article at www.ajnr.org.

REFERENCES

1. FDA clears first 7T magnetic resonance imaging device. https://www.fda.gov/news-events/press-announcements/fda-clears-first-7t-magnetic-resonance-imaging-device. Accessed January 11, 2023
2. **Bringing Ultra-High Field MR Imaging from Research to Clinical: SIGNA 7.0T FDA Cleared.** https://www.gehealthcare.com/about/newsroom/press-releases/bringing-ultra-high-field-mr-imaging-from-research-to-clinical-signa-70t-fda-cleared?npclid=botnpclid. Accessed December 12, 2023
3. Özütemiz C, White M, Elvendahl W, et al. **Use of a commercial 7-T MRI scanner for clinical brain imaging: indications, protocols, challenges, and solutions-a single-center experience**. *AJR Am J Roentgenol* 2023;221:788–804 CrossRef Medline
4. Okada T, Fujimoto K, Fushimi Y, et al. **Neuroimaging at 7 Tesla: a pictorial narrative review.** *Quant Imaging Med Surg* 2022;12:3406–35 CrossRef Medline
5. Opheim G, van der Kolk A, Markenroth Bloch K, et al. **7T epilepsy task force consensus recommendations on the use of 7T MRI in clinical practice.** *Neurology* 2021;96:327–41 CrossRef Medline
6. Ugurbil K. **Magnetic resonance imaging at ultrahigh fields.** *IEEE Trans Biomed Eng* 2014;61:1364–79 CrossRef Medline
7. Grams AE, Kraff O, Kalkmann J, et al. **Magnetic resonance imaging of cranial nerves at 7 Tesla.** *Clin Neuroradiol* 2013;23:17–23 CrossRef Medline
8. Lecler A, Duron L, Charlson E, et al. **Comparison between 7 Tesla and 3 Tesla MRI for characterizing orbital lesions.** *Diagn Interv Imaging* 2022;103:433–39 CrossRef Medline
9. Ma R, Henry TR, Van de Moortele PF. **Eliminating susceptibility induced hyperintensities in T1w MPRAGE brain images at 7T.** *Magn Reson Imaging* 2019;63:274–79 CrossRef Medline
10. Snaar JE, Teeuwisse WM, Versluis MJ, et al. **Improvements in high-field localized MRS of the medial temporal lobe in humans using new deformable high-dielectric materials.** *NMR Biomed* 2011;24:873–79 CrossRef Medline
11. Teeuwisse WM, Brink WM, Webb AG. **Quantitative assessment of the effects of high-permittivity pads in 7 Tesla MRI of the brain.** *Magn Reson Med* 2012;67:1285–93 CrossRef Medline
12. Van de Moortele PF, Akgun C, Adriany G, et al. **B(1) destructive interferences and spatial phase patterns at 7 T with a head transceiver array coil.** *Magn Reson Med* 2005;54:1503–18 CrossRef Medline
13. Yang QX, Mao W, Wang J, et al. **Manipulation of image intensity distribution at 7.0 T: passive RF shimming and focusing with dielectric materials.** *J Magn Reson Imaging* 2006;24:197–202 CrossRef Medline
14. Eisenhut F, Schlaffer SM, Hock S, et al. **Ultra-high-field 7 T magnetic resonance imaging including dynamic and static contrast-enhanced T1-weighted imaging improves detection of secreting pituitary microadenomas.** *Invest Radiol* 2022;57:567–74 CrossRef Medline
15. Patel V, Liu CJ, Shiroishi MS, et al. **Ultra-high field magnetic resonance imaging for localization of corticotropin-secreting pituitary adenomas.** *Neuroradiology* 2020;62:1051–54 CrossRef Medline
16. Rutland JW, Delman BN, Feldman RE, et al. **Utility of 7 Tesla MRI for preoperative planning of endoscopic endonasal surgery for pituitary adenomas.** *J Neurol Surg B Skull Base* 2021;82:303–12 CrossRef Medline
17. Yao A, Rutland JW, Verma G, et al. **Pituitary adenoma consistency: direct correlation of ultrahigh field 7T MRI with histopathological analysis.** *Eur J Radiol* 2020;126:108931 CrossRef Medline
18. Mark IT, Welker K, Erickson D, et al. **7T MRI for Cushing's disease: a single institutional experience and literature review**. *AJNR Am J Neuroradiol* 2024;45:971–76 CrossRef Medline
19. Snaar JE, Teeuwisse WM, Versluis MJ, et al. **Improvements in high-field localized MRS of the medial temporal lobe in humans using new deformable high-dielectric materials.** *NMR Biomed* 2011;24:873–79 CrossRef Medline
20. Fagan AJ, Bitz AK, Bjorkman-Burtscher IM, et al; ISMRM Safety Committee. **7T MR safety.** *J Magn Reson Imaging* 2021;53:333–46 CrossRef Medline
21. Castillo M. **Pituitary gland: development, normal appearances, and magnetic resonance imaging protocols.** *Top Magn Reson Imaging* 2005;16:259–68 CrossRef Medline
22. Tortori-Donati P, Rossi A, Biancheri R. **Sellar and Suprasellar Disorders**. In: Tortori-Donati P, ed. *Pediatric Neuroradiology*. Heidelberg: Springer-Verlag 2005: 855–92
23. Raybaud C, Barkovich AJ. **Rathke Cleft Cysts**. In: Raybaud C, Barkovich AJ, eds. *Pediatric Neuroimaging*. Philadelphia: Lippincott Williams & Wilkins; 2012:733–34
24. Osborn AG. **Rathke Cleft Cyst**. In: Osborn AG, ed. *Brain*. Manitoba, Canada: Amirsys; 2013: 682–99
25. Mahdi ES, Webb RL, Whitehead MT. **Prevalence of pituitary cysts in children using modern magnetic resonance imaging techniques.** *Pediatr Radiol* 2019;49:1781–87 CrossRef Medline
26. Gobara A, Katsube T, Asou H, et al. **T2 hypointense signal discovered incidentally at the posterior edge of the adenohypophysis on MRI: its prevalence and morphology and their relationship to age.** *Neuroradiology* 2022;64:1755–61 CrossRef Medline
27. Mendoza JW, Strickland BA, Micko A, et al. **Prevalence rate of coexisting Rathke cleft cysts and pineal cysts: a multicenter**

cross-sectional study. *World Neurosurg* 2021;149:e455–59 CrossRef Medline
28. Larkin S, Karavitaki N, Ansorge O. **Rathke's cleft cyst**. In: Fliers E, Korbonits M, Romijn JA, eds. *Handbook of Clinical Neurology*. Amsterdam, Netherlands: Elsevier; 2014:255–69
29. Schmidt B, Cattin F, Aubry S. **Prevalence of Rathke cleft cysts in children on magnetic resonance imaging.** *Diagn Interv Imaging* 2020;101:209–15 CrossRef Medline
30. Famini P, Maya MM, Melmed S. **Pituitary magnetic resonance imaging for sellar and parasellar masses: ten-year experience in 2598 patients.** *J Clin Endocrinol Metab* 2011;96:1633–41 CrossRef Medline
31. Hoang JK, Hoffman AR, González RG, et al. **Management of Incidental Pituitary Findings on CT, MRI, and ^{18}F-Fluorodeoxyglucose PET: A White Paper of the ACR Incidental Findings Committee**. *J Am Coll Radiology* 2018;15:966–72 CrossRef Medline